Electronic Supporting Information

for

Hydrolytic instability of C–F bonds in 2,2,2-trifluoroethyl-phosphinic acid systems: formation of carboxymethylphosphinic acid derivatives

Filip Koucký [a], Ivana Císařová [a] and Jan Kotek [a,*]

[a] Department of Inorganic Chemistry, Faculty of Science, Charles University, Hlavova 8, 128 42 Prague 2, Czech Republic. E-mail: modrej@natur.cuni.cz.

Contents

Synthesis and crystal structures

N-(2,2,2-trifluoroethyl)morpholine (16)

The compound was previously prepared by a reductive process involving phenylsilane,[1] alkylation mediated by SO_2F_2 [2] or employing an Ar-plasma microreactor.[3] To find a more available and convenient method, we used a reduction of the amide group in *N*-trifluoroacetyl-morpholine to the corresponding amine **16**, analogously to the procedure used in syntheses of other *N*-trifluoroethyl derivatives which we studied previously, using BH_3 generated *in situ* by reaction of $NaBH_4$ and $BF_3{\cdot}Et_2O$ in etheric solvent.[4,5] The final yield 27% is relatively low due to partial solubility in the used solvent (H_2O, MeOH, Et_2O). Synthesis proceeded according to Scheme S1.

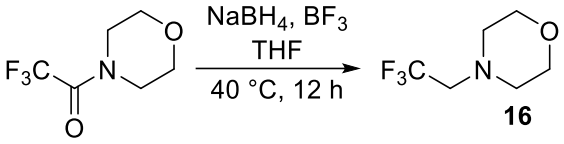

Scheme S1. Synthesis of *N*-(2,2,2-trifluoroethyl)morpholine **16**.

Crystallisation by Et_2O vapour diffusion into a solution of **16** in aq. HCl:MeOH mixture afforded single crystals of **16**·HCl suitable for X-ray diffraction analysis (Figure S1).

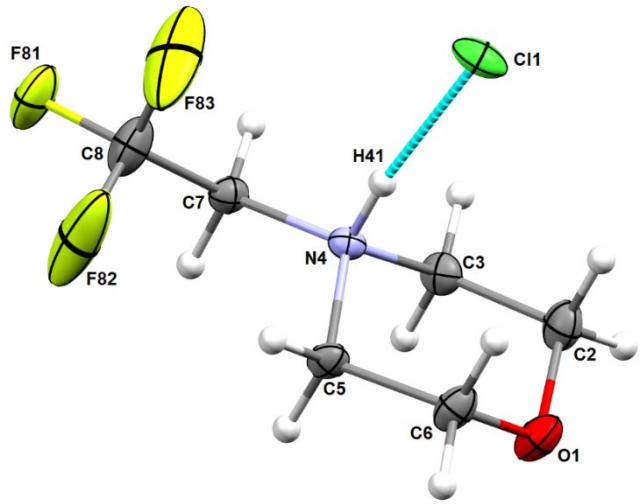

Figure S1. Structurally independent part found in the crystal structure of **16**·HCl. A hydrogen bond between the protonated amino group and the chloride anion is shown in turquoise.

Detailed description of synthesis of N-(2,2,2-trifluoroethyl)morpholine (16)

$NaBH_4$ (2.10 g, 55.3 mmol, 5.0 equiv.) was added into a 250 mL three-neck flask equipped with an inert gas (N_2) inlet, a septum and a gas bubbler filled with nujol. The apparatus was flushed with N_2, and *N*-(2,2,2-trifluoroacetyl)morpholine (2.00 g, 10.9 mmol, 1.0 equiv.) dissolved in anhydrous THF (distillation from Na, 20 mL) was injected through the septum into the flask. The mixture was diluted

with anhydrous THF (40 mL) and was heated to 40 °C under a gentle stream of N_2. Then, $BF_3{\cdot}Et_2O$ (3.4 mL, 27.5 mmol, 2.5 equiv.) was injected through the septum into the reaction mixture. The outgoing gases were bubbled through a gas bubbler filled with nujol and passed through an aq. solution of NaOH (10%) and H_2O_2 (5%). The reaction mixture was stirred at 40 °C under a very gentle nitrogen stream overnight. After this period, the reaction was quenched by the addition of 1 M HCl (25 mL), and volatiles were evaporated using a vacuum rotary evaporator. The residue was transferred into a 250mL separation funnel and separated between dichloromethane (100 mL) and 5% aq. NaOH (100 mL). The organic layer was separated, the solvent was evaporated, and the residue was treated with 1 M HCl (50 mL). The mixture was evaporated, and the residue was dissolved in a small amount of water and evaporated again. The residue was dissolved in MeOH (10 mL), and the solvent was allowed to evaporate freely. The formed crystals were washed with Et_2O and collected. Yield of hydrochloride **16**·HCl was 0.60 g (27%).

Elemental analysis: found (calc. for $C_6H_{11}NOF_3Cl$, M_r = 205.6) C: 34.67 (35.05), H: 5.10 (5.39), N: 6.46 (6.81), F: 27.88 (27.72), Cl: 17.56 (17.24).

NMR: (D_2O, pD 1.8): ^{1}H: 3.56 (4H, t, NCH_2CH$_2$ $^3J_{HH}$ = 3.6); 4.03 (4H, t, OCH_2CH$_2$, $^3J_{HH}$ = 4.0); 4.18 (2H, q, NCH_2CF$_3$, $^3J_{HF}$ = 8.9). ^{13}C{^{1}H} 53.8 (s, N*C*H$_2$CH$_2$); 56.4 (q, N*C*H$_2$CF$_3$, $^2J_{CF}$ = 34); 64.1 (s, O*C*H$_2$CH$_2$); 122.6 (q, *C*F$_3$, $^1J_{CF}$ = 278). ^{19}F: –65.30 (t, $^3J_{FH}$ = 8.9). See Figures S13–S15.

Single crystals for X-ray analysis were obtained by Et_2O vapour diffusion into the MeOH/HCl solution of **16**·HCl.

Tris{[2,2,2-trifluoroethyl(hydroxy)phosphoryl]methyl}amine (17)

During the synthesis of 2,2,2-trifluoroethyl(hydroxymethyl)phosphinic acid **5** by reaction of 2,2,2-trifluoroethylphosphinic acid with formaldehyde, tris{[2,2,2-trifluoroethyl(hydroxy)phosphoryl]methyl}amine **17** was formed as a by-product if some traces of ammonia were present in the reaction mixture (Scheme S2; Scheme 3 in the main text). The solubility of this compound is low, and it crystallised from the evaporated reaction mixture, whereas the main product – hydroxymethyl(2,2,2-trifluoroethyl)phosphinic acid **5** – is a colourless oil. When occasionally present, a small amount of solid by-product **17** was isolated by vacuum filtration and re-crystallised from boiling water to obtain suitable single crystals and its identity was confirmed by X-ray diffraction analysis (Figure S2). In the molecular structure, the amino group is surprisingly non-protonated, whereas all phosphinic acid pendant arms are protonated, and their protonations are stabilised by very strong hydrogen bonds [d(O–H···O) ≈ 2.5 Å] to the phosphoryl oxygen atoms of the neighbouring molecules of **17**. It points to a very low basicity of the amino group due to the presence of three phosphinic acid moieties with strong electron-withdrawing properties.

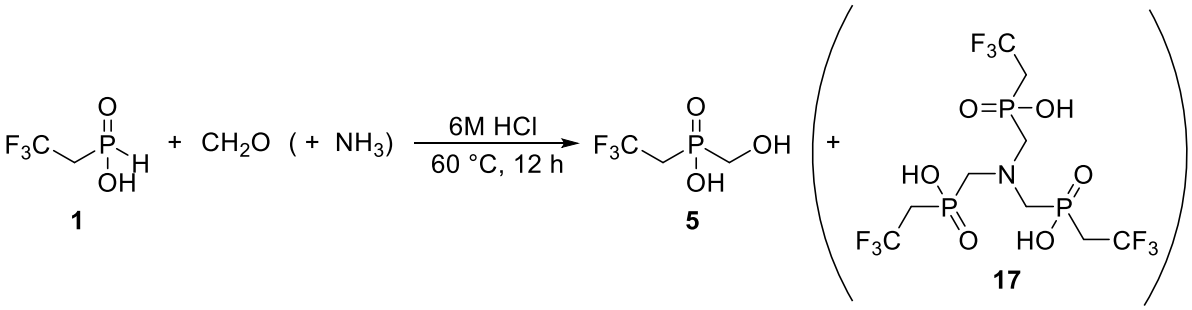

Scheme S2. Synthesis of hydroxymethyl(2,2,2-trifluoroethyl)phosphinic acid **5** showing formation of tris{[2,2,2-trifluoroethyl(hydroxy)phosphoryl]methyl}amine **17** as the by-product if traces of ammonia were present in the reaction mixture.

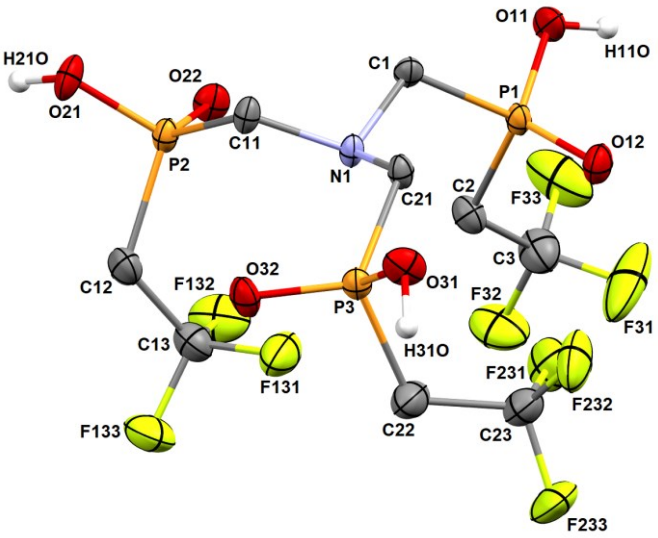

Figure S2. The molecular structure of tris[methylene(2,2,2-trifluoroethylphosphinic acid)] **17** found in its crystal structure. Carbon-bound hydrogen atoms are omitted for the sake of clarity. The trifluoroethyl group attached to the phosphorus atom P3 was found to be disordered in two close positions with almost overlaying carbon atoms C23a/b and staggered trifluoromethyl groups. These two different possibilities had occupancies 83:17%, and only a variant with the higher occupancy is shown.

Characterisation NMR spectra of new compounds

2,2,2-Trifluoroethyl(hydroxymethyl)phosphinic acid (5)

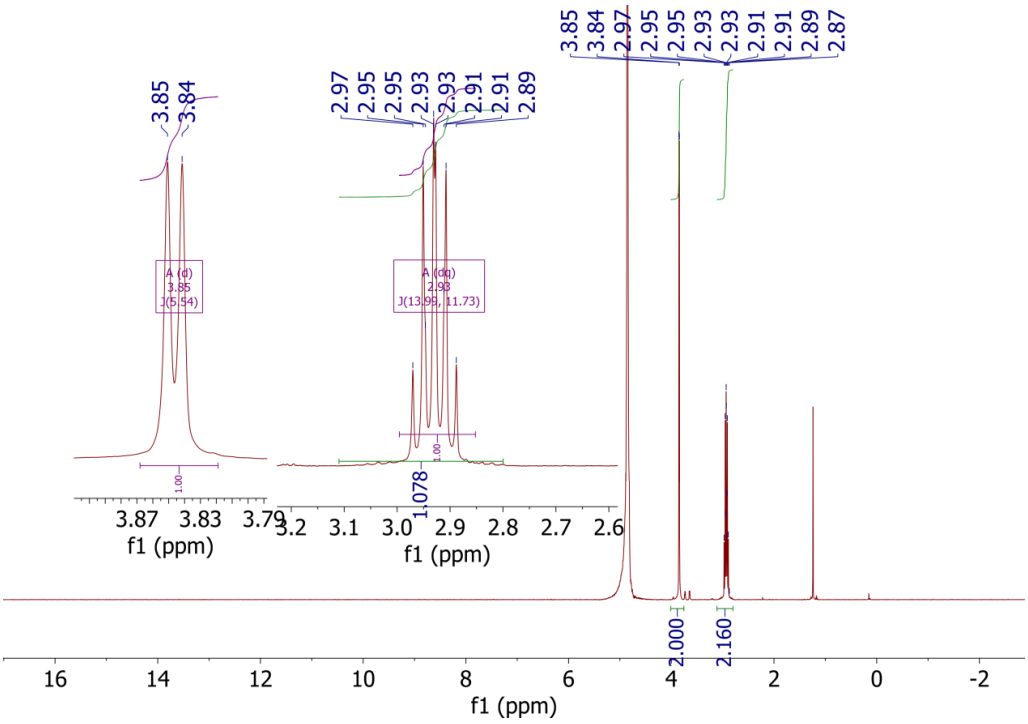

Figure S3. ^{1}H NMR spectrum of **5**. *t*BuOH reference in insert (1.24 ppm), 600 MHz, 25 °C, D_2O, pD 0.6.

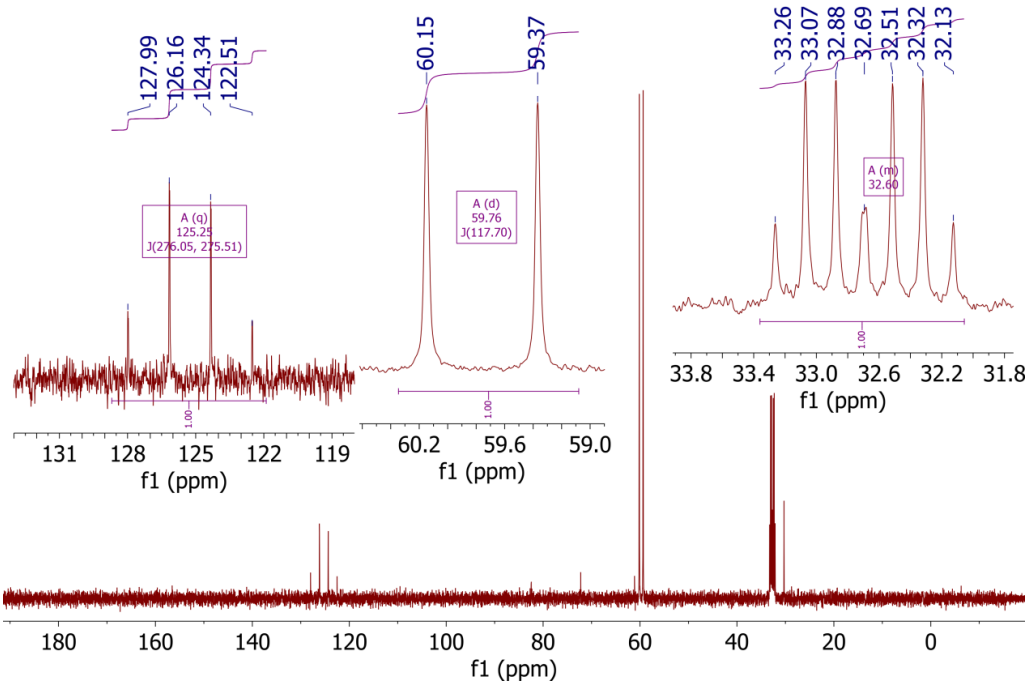

Figure S4. $^{13}C\{^{1}H\}$ NMR spectrum of **5**. *t*BuOH reference in insert (30.29 ppm), 151 MHz, 25 °C, D_2O, pD 0.6.

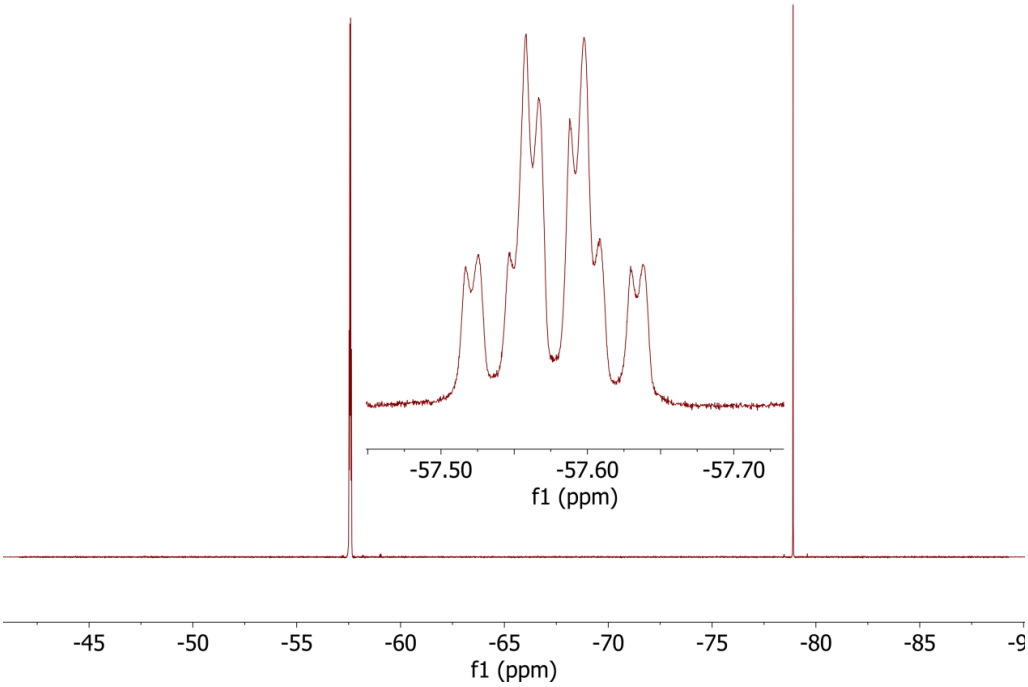

Figure S5. ^{19}F NMR spectrum of **5**. Triflic acid reference in insert (−78.9 ppm), 282 MHz, 25 °C, D_2O, pD 0.6.

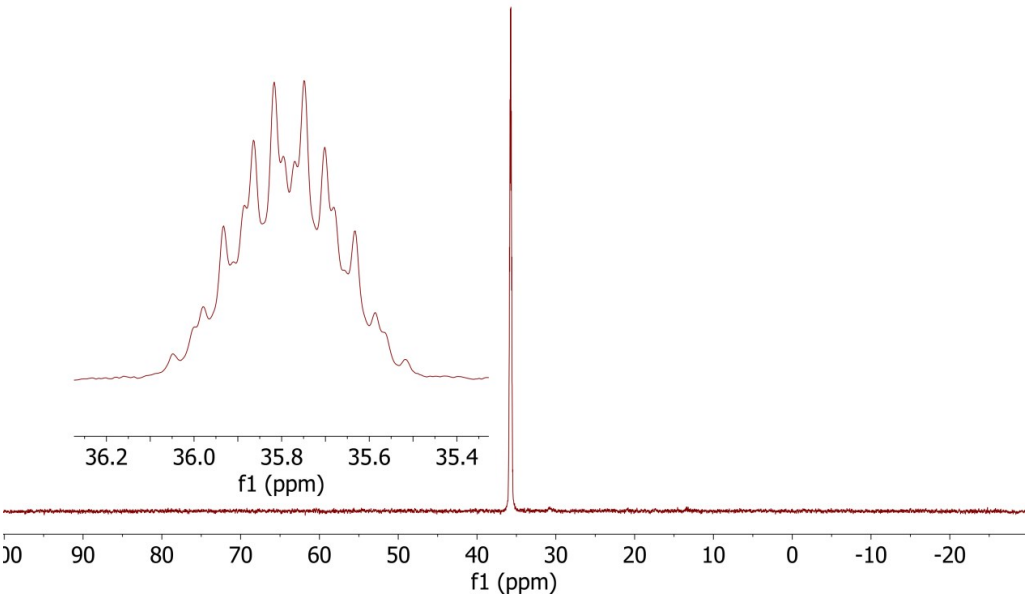

Figure S6. ^{31}P NMR spectrum of **5**. 121 MHz, 25 °C, D_2O, pD 0.6.

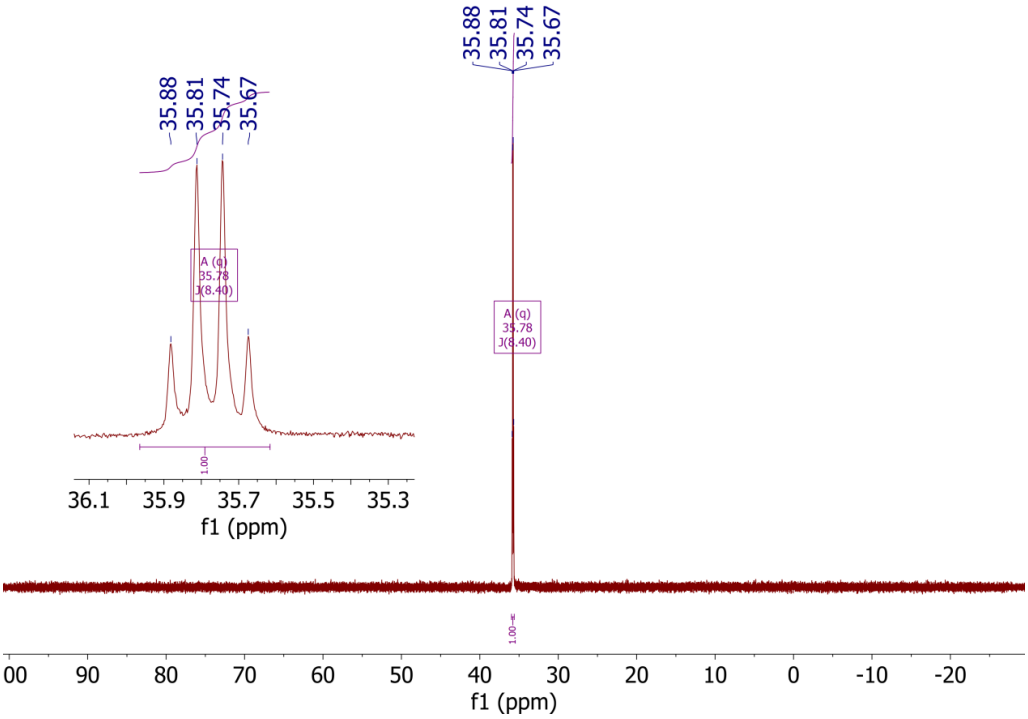

Figure S7. $^{31}P[^{1}H]$ NMR spectrum of **5**. 121 MHz, 25 °C, D_2O, pD 0.6.

2,2,2-Trifluoroethylphosphonic acid (6)

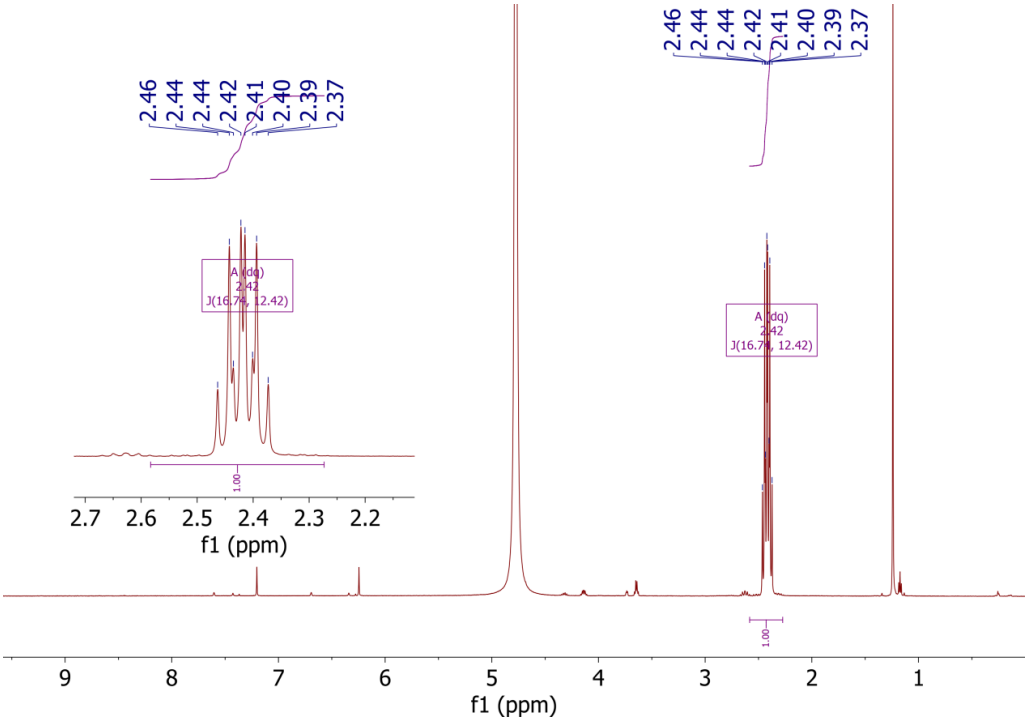

Figure S8. ^{1}H NMR spectrum of **6**. *t*BuOH reference in insert (1.24 ppm), 600 MHz, 25 °C, D_2O, pD 7.5.

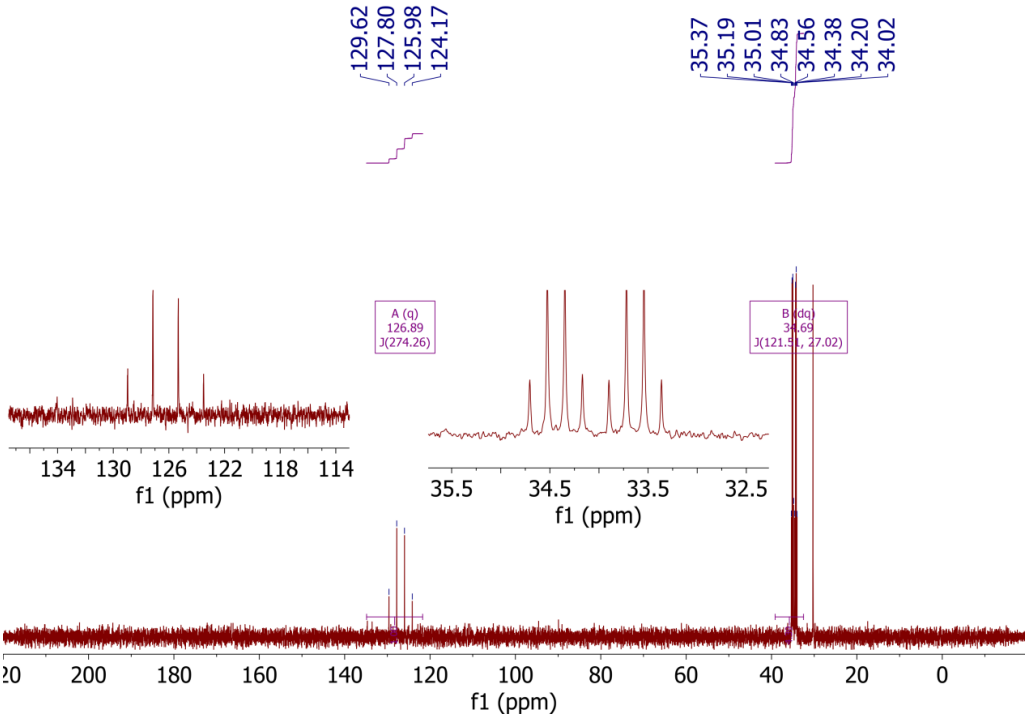

Figure S9. $^{13}C\{^{1}H\}$ NMR spectrum of **6**. *t*BuOH reference in insert (30.29 ppm), 151 MHz, 25 °C, D_2O, pD 7.5.

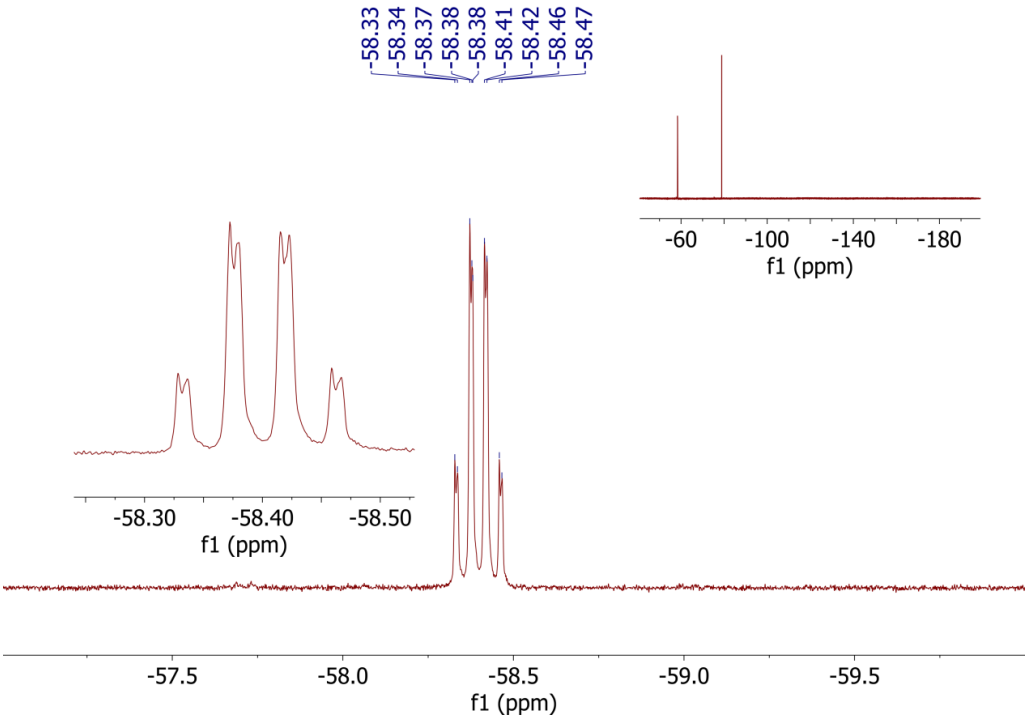

Figure S10. ^{19}F NMR spectrum of **6**. Triflic acid reference in insert (−78.9 ppm), 282 MHz, 25 °C, D_2O, pD 7.5.

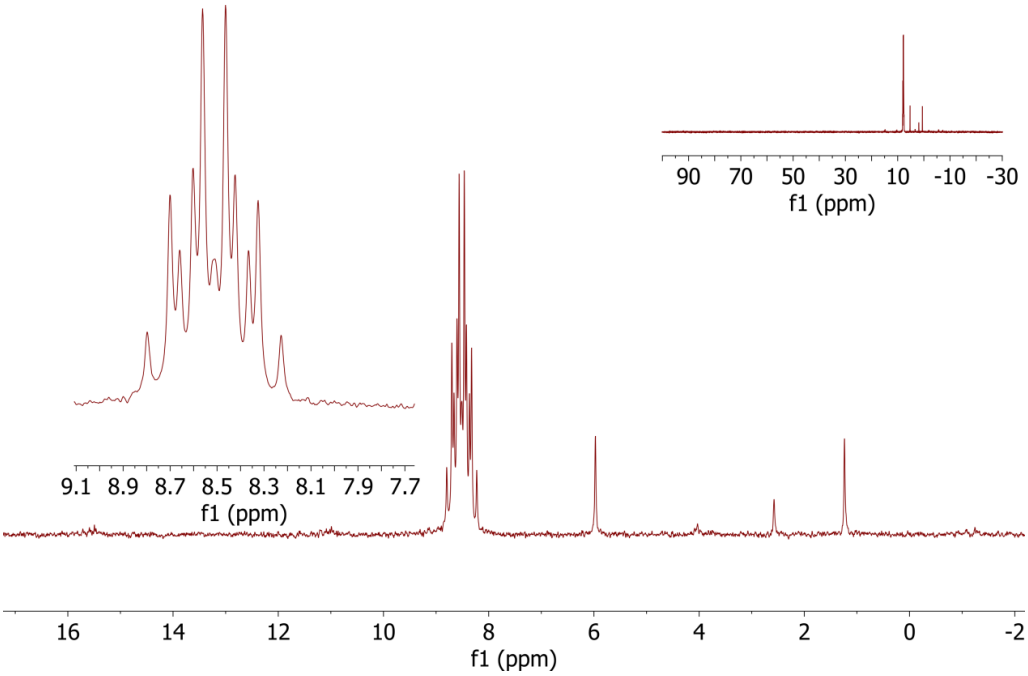

Figure S11. ^{31}P NMR spectrum of **6**. 121 MHz, 25 °C, D_2O, pD 7.5.

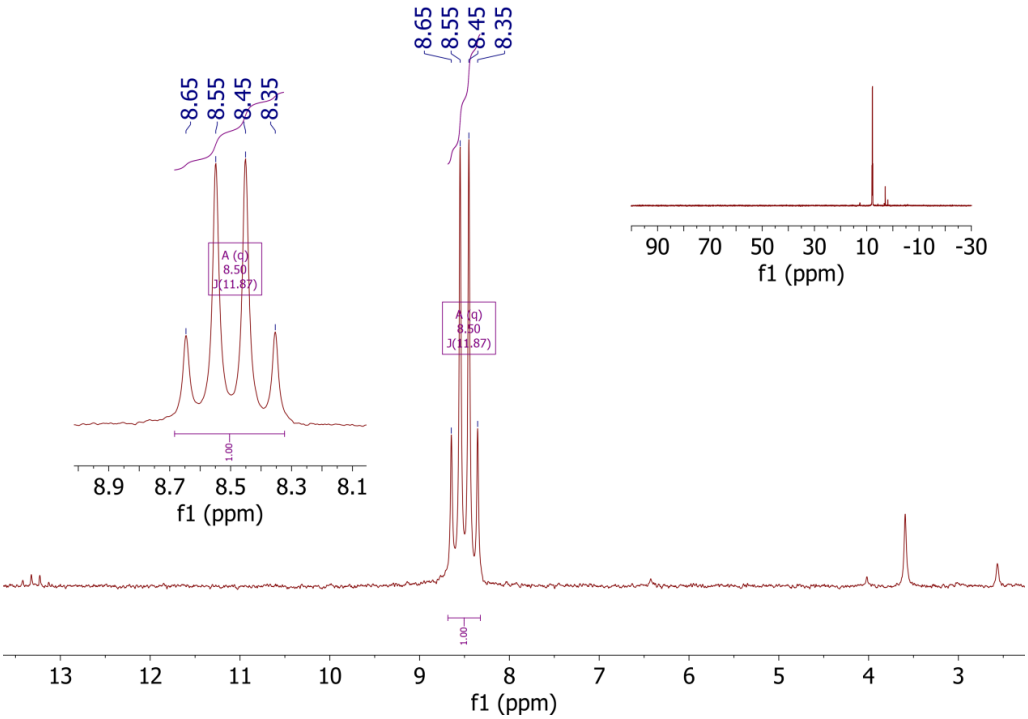

Figure S12. $^{31}P\{^{1}H\}$ NMR spectrum of **6**. 121 MHz, 25 °C, D_2O, pD 7.5.

***N*-(2,2,2-Trifluoroethyl)morpholine (16)**

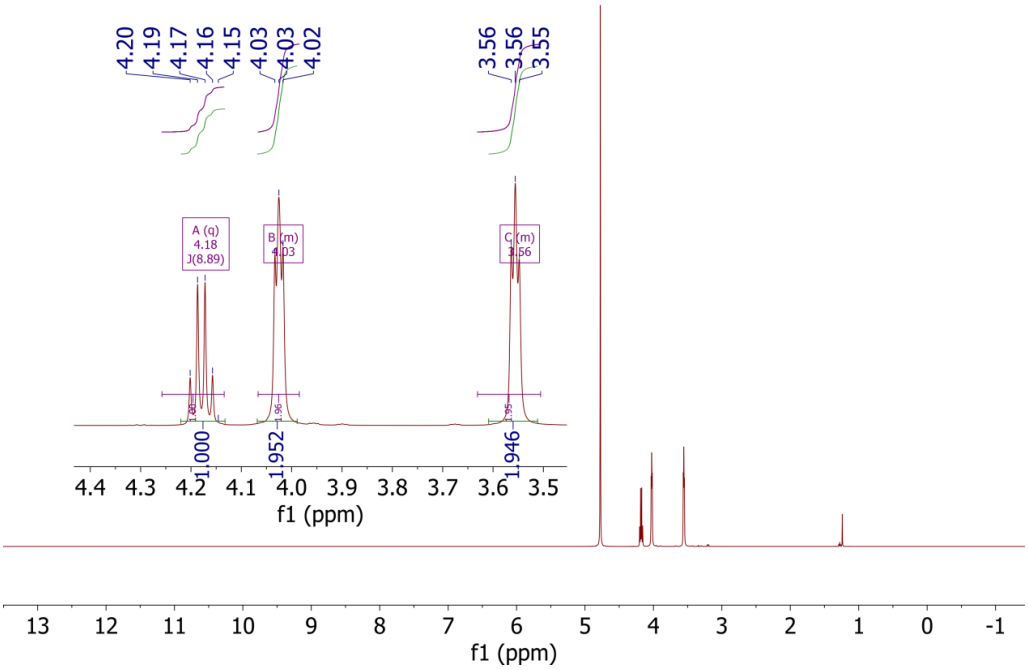

Figure S13. ^{1}H NMR spectrum of **16**. *t*BuOH reference in insert (1.24 ppm), 600 MHz, 25 °C, D_2O, pD 1.8.

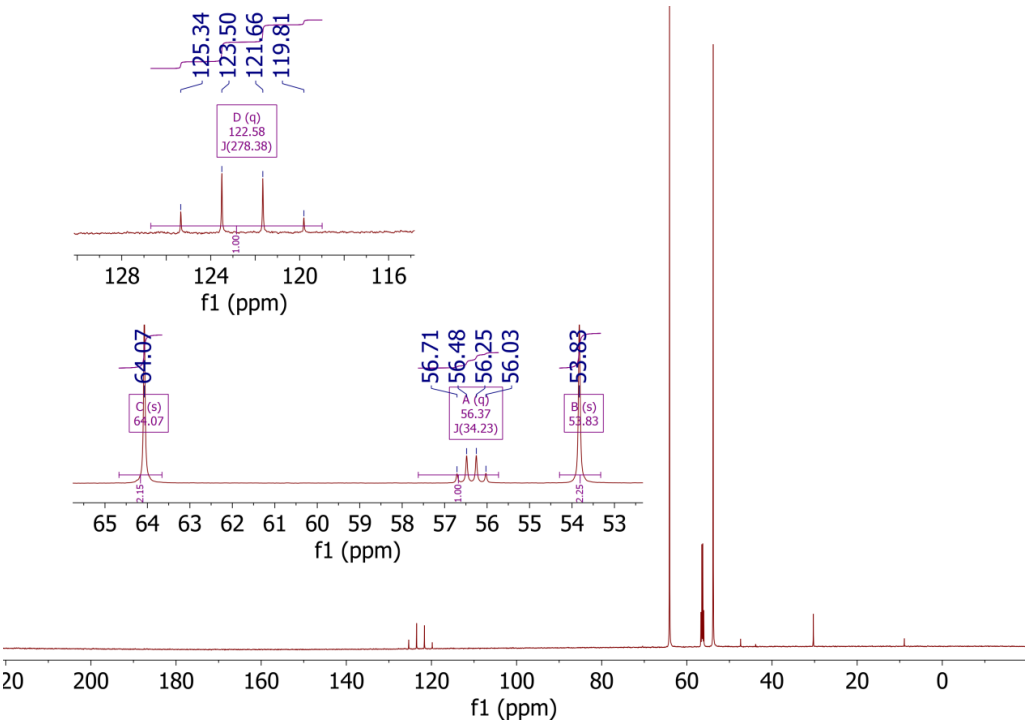

Figure S14. $^{13}C\{^{1}H\}$ NMR spectrum of **16**. *t*BuOH reference in insert (30.29 ppm), 151 MHz, 25 °C, D_2O, pD 1.8.

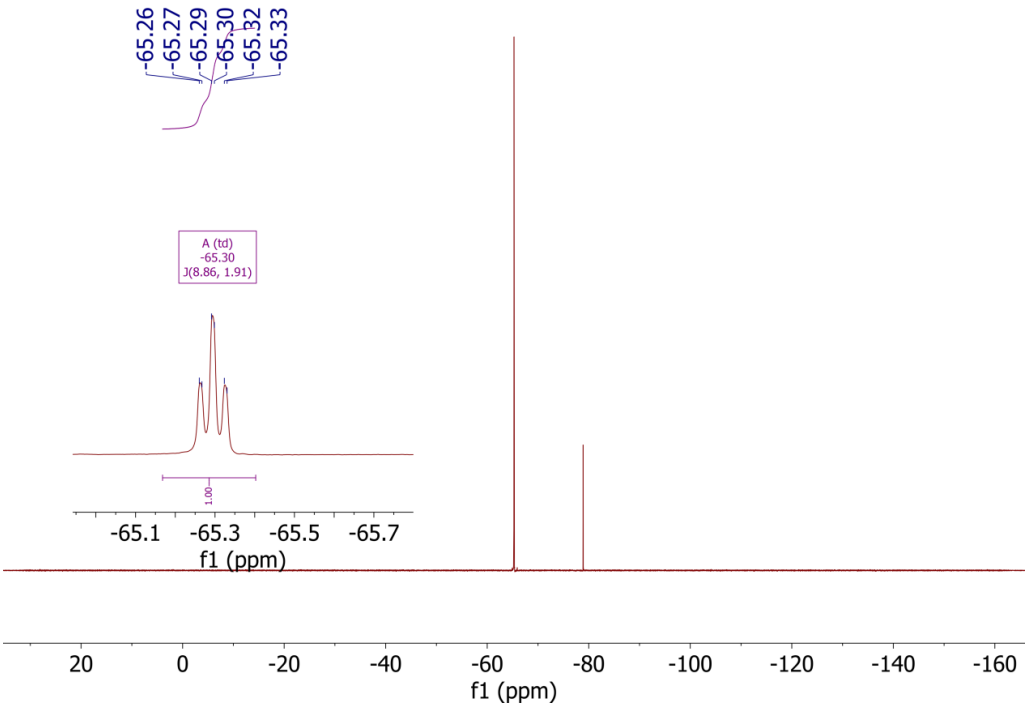

Figure S15. ^{19}F NMR spectrum of **16**. Triflic acid reference in insert (−78.9 ppm), 282 MHz, 25 °C, D_2O, pD 1.8.

Hydrolytic experiments followed by ^{19}F NMR spectroscopy

Basic hydrolysis of 2

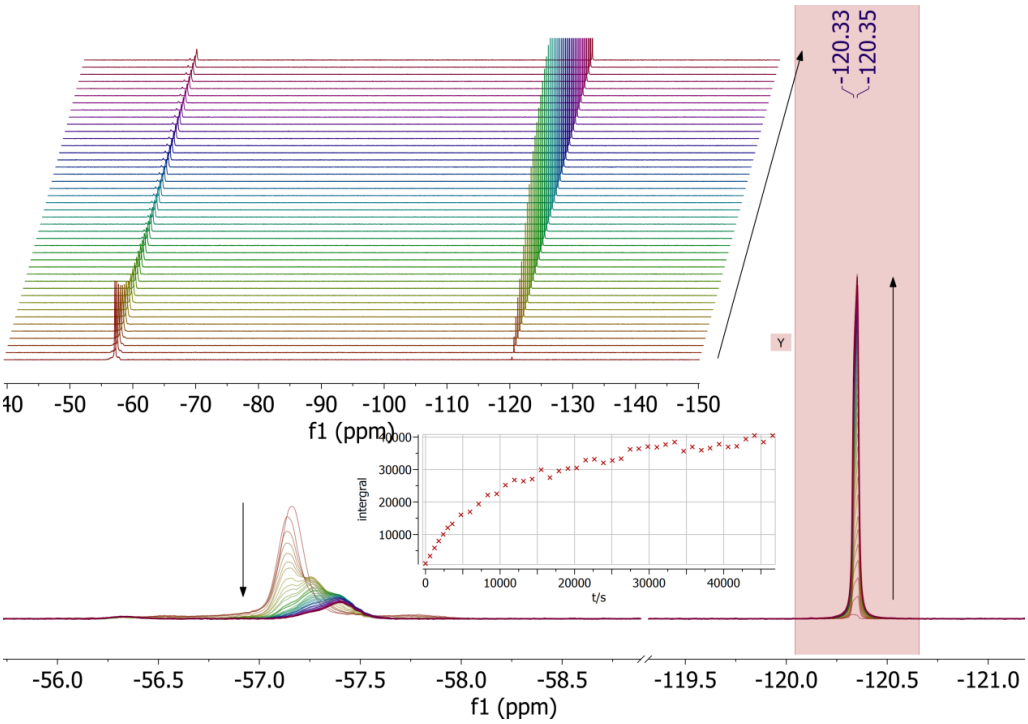

Figure S16. ^{19}F NMR PAD spectra showing hydrolysis of **2** in a strongly alkaline solution (starting pH 11) and formation of fluoride. 282 MHz, 50 °C, duration 14 h.

Basic hydrolysis of 3

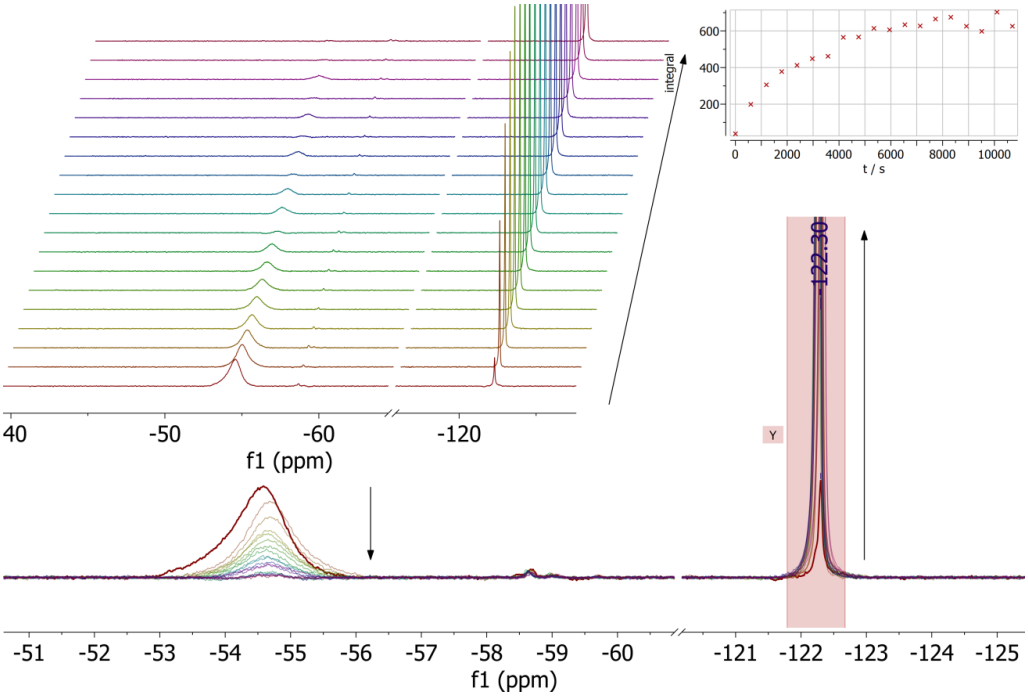

Figure S17. ^{19}F NMR PAD spectra showing hydrolysis of **3** in a strongly alkaline solution (starting pH 11) and formation of fluoride. 282 MHz, 50 °C, duration 3 h.

Basic hydrolysis of 4

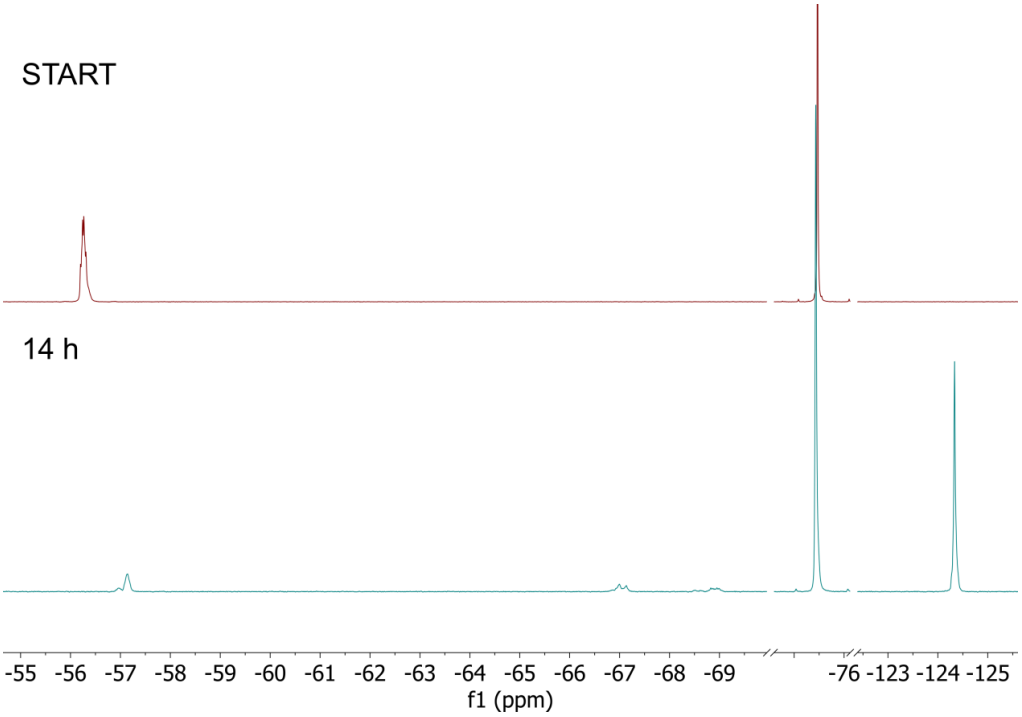

Figure S18. ^{19}F NMR spectra showing hydrolysis of **4** in a strongly alkaline solution (starting pH 11) and formation of fluoride. 282 MHz, 25 °C, hydrolysis was completed overnight, and side reactions were observed.

Basic hydrolysis of 5

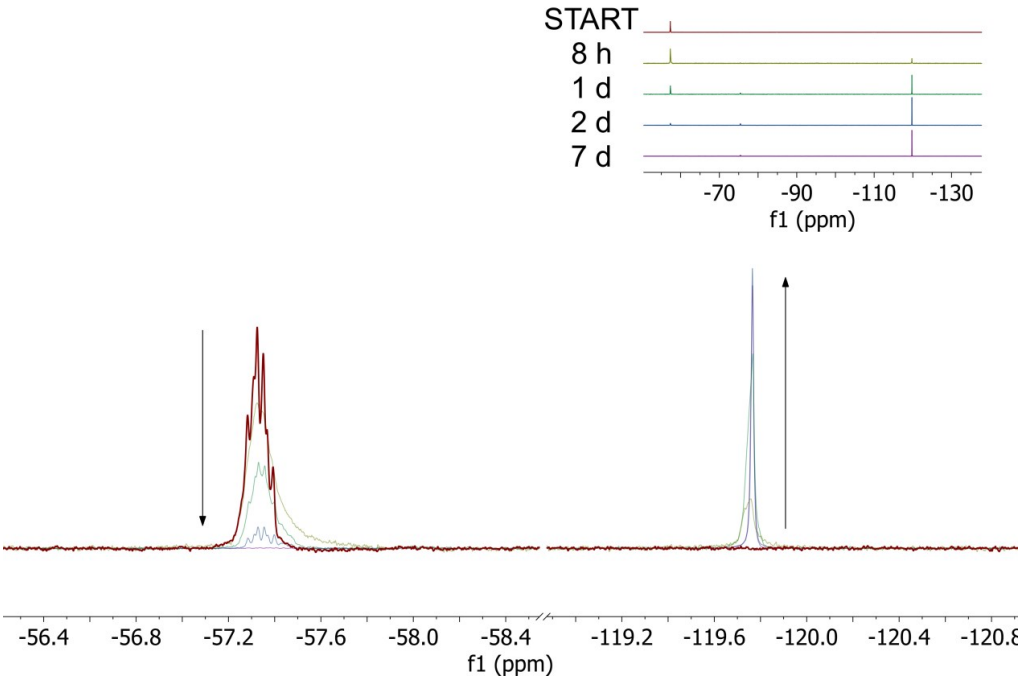

Figure S19. ^{19}F NMR spectra showing hydrolysis of **5** in a strongly alkaline solution (starting pH 11) and formation of fluoride. 282 MHz, 25 °C.

Trial to hydrolyse 6

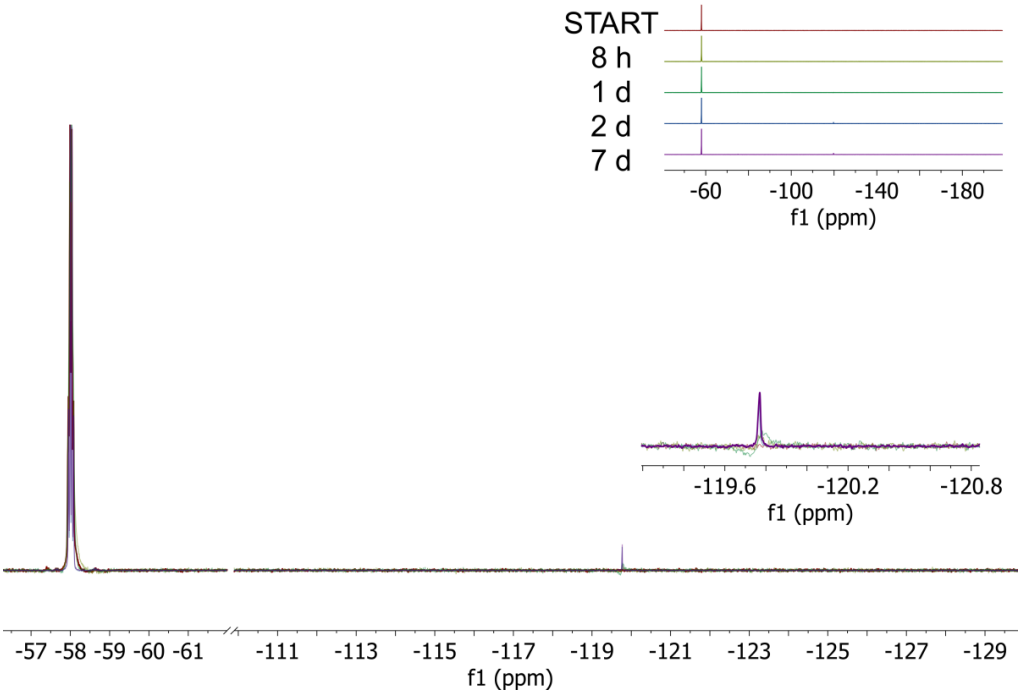

Figure S20. ^{19}F NMR spectra showing hydrolytic stability of **6** in a strongly alkaline solution (pH 11). 282 MHz, 25 °C. A very small signal of the fluoride ions comes from the hydrolysis of traces of impurities (compound **1**) present in the sample.

Basic hydrolysis of 7

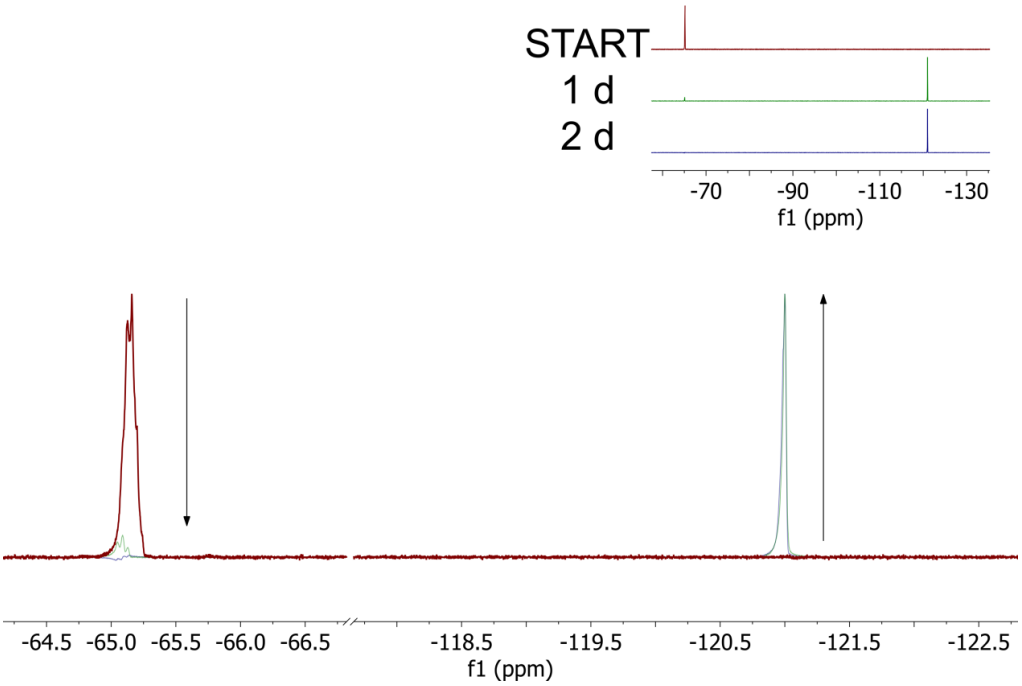

Figure S21. ^{19}F NMR spectra showing hydrolysis of **7** in a strongly alkaline solution (starting pH 11) and formation of fluoride. 282 MHz, 25 °C.

Trial to hydrolyse 8

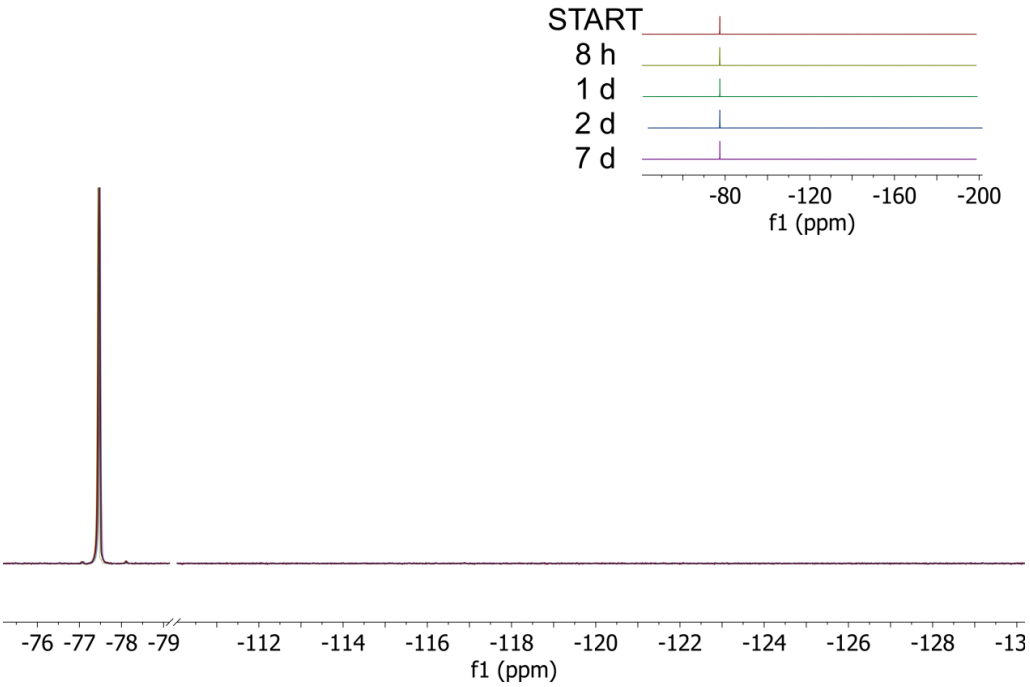

Figure S22. ^{19}F NMR spectra showing hydrolytic stability of **8** in a strongly alkaline solution (pH 11). 282 MHz, 25 °C.

Trial to hydrolyse 9

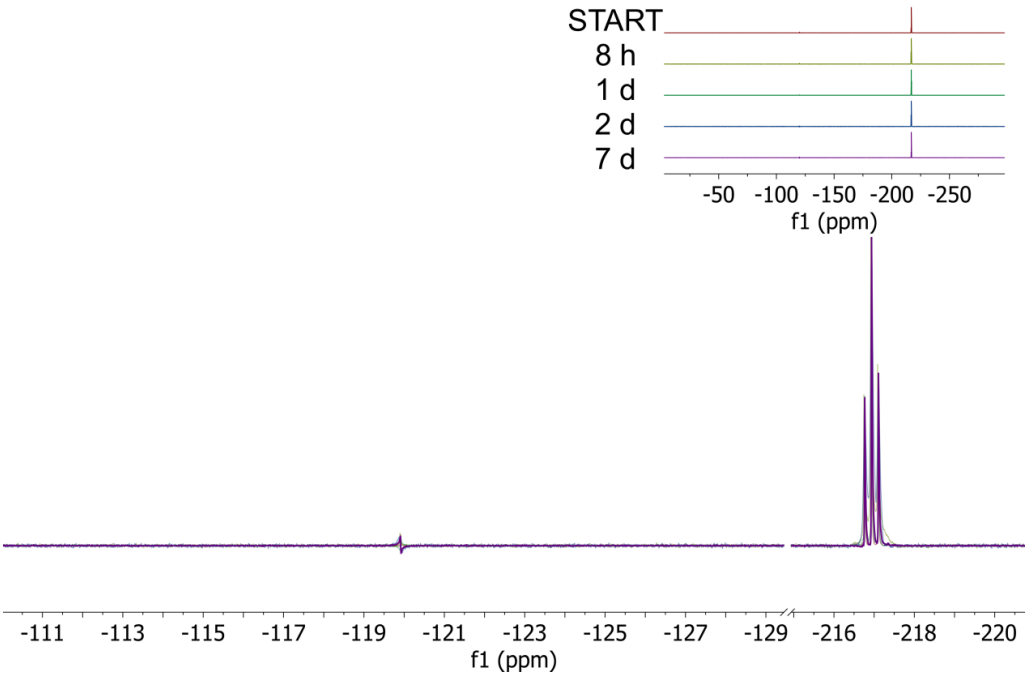

Figure S23. ^{19}F NMR spectra showing hydrolytic stability of **9** in a strongly alkaline solution (pH 11). 282 MHz, 25 °C.

Trial to hydrolyse 10

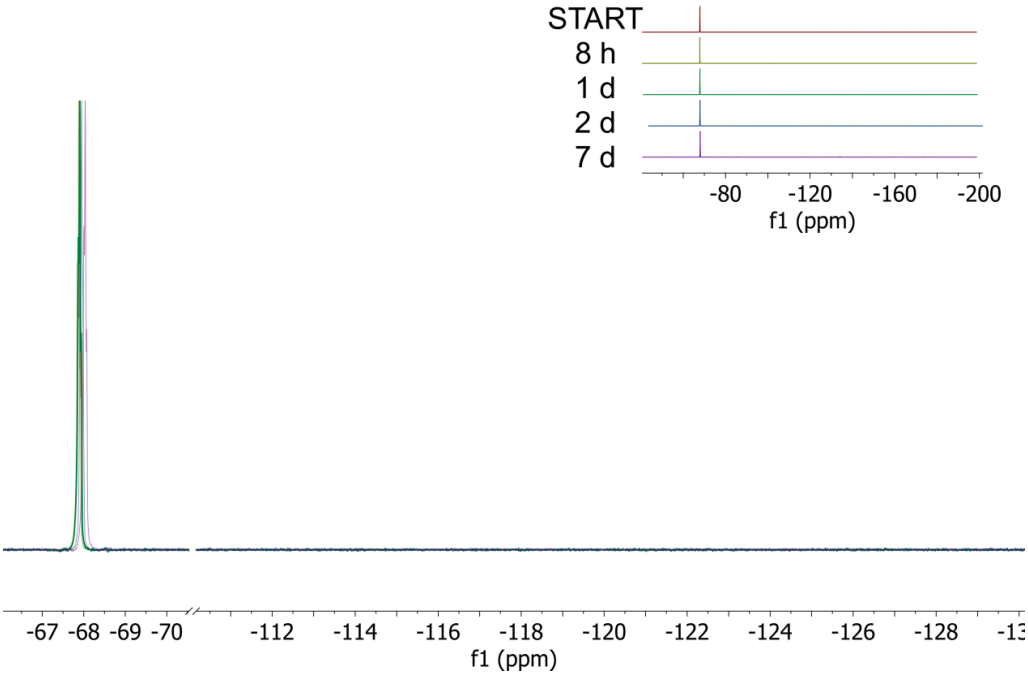

Figure S24. ^{19}F NMR spectra showing hydrolytic stability of **10** in a strongly alkaline solution (pH 11). 282 MHz, 25 °C.

Trial to hydrolyse 11

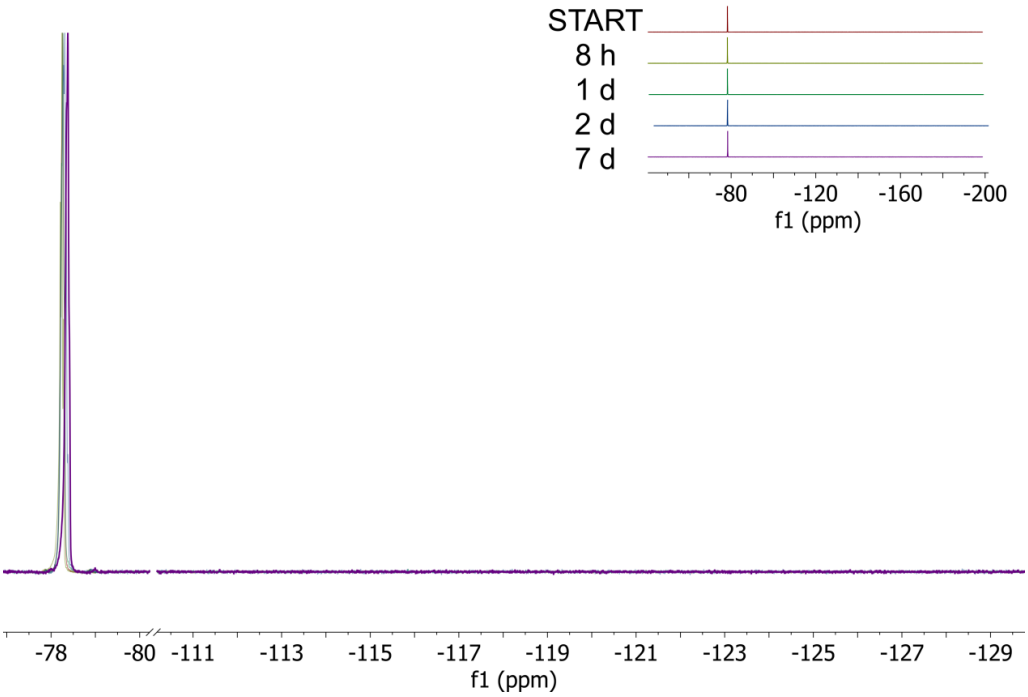

Figure S25. ^{19}F NMR spectra showing hydrolytic stability of **11** in a strongly alkaline solution (pH 11). 282 MHz, 25 °C.

Trial to hydrolyse 12

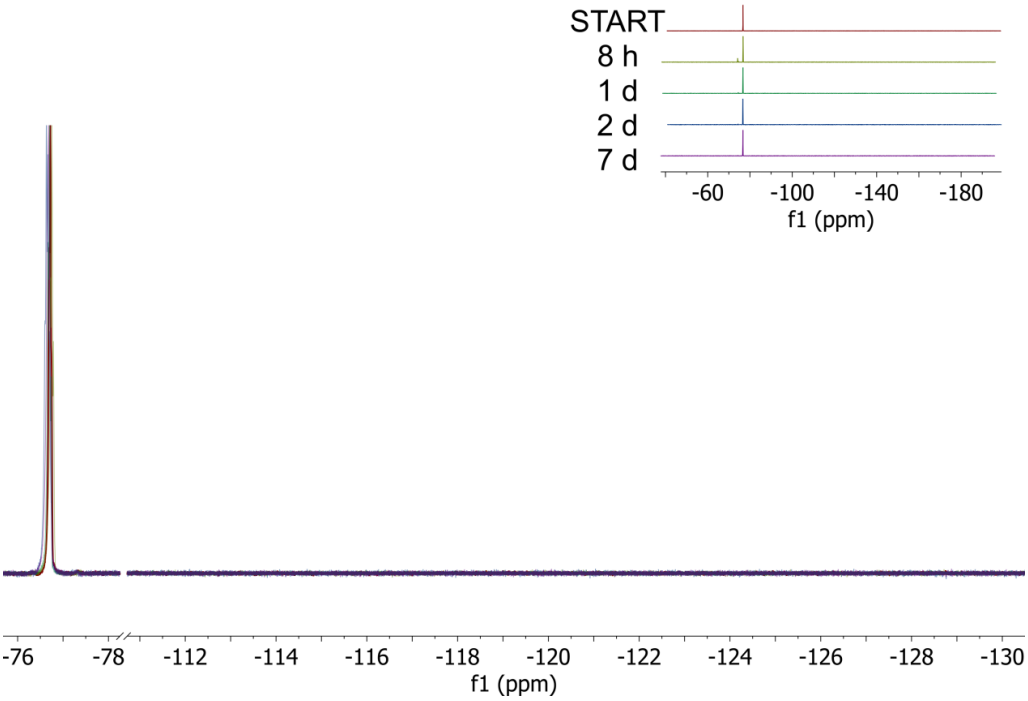

Figure S26. ^{19}F NMR spectra showing hydrolytic stability of **12** in a strongly alkaline solution (pH 11). 282 MHz, 25 °C.

Trial to hydrolyse 13

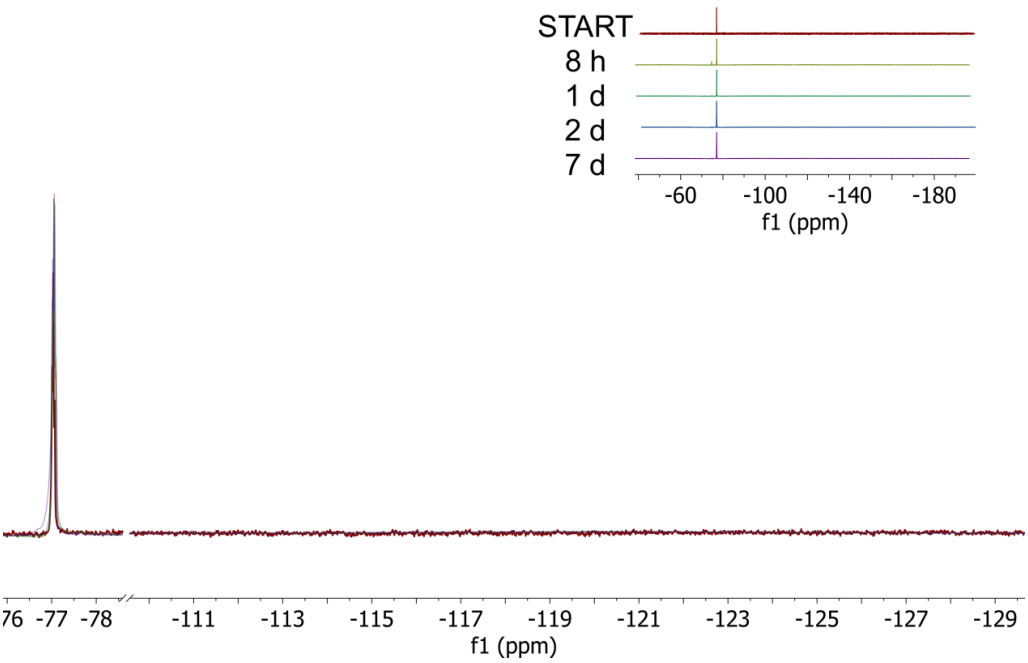

Figure S27. ^{19}F NMR spectra showing hydrolytic stability of **13** in a strongly alkaline solution (pH 11). 282 MHz, 25 °C.

Trial to hydrolyse 14

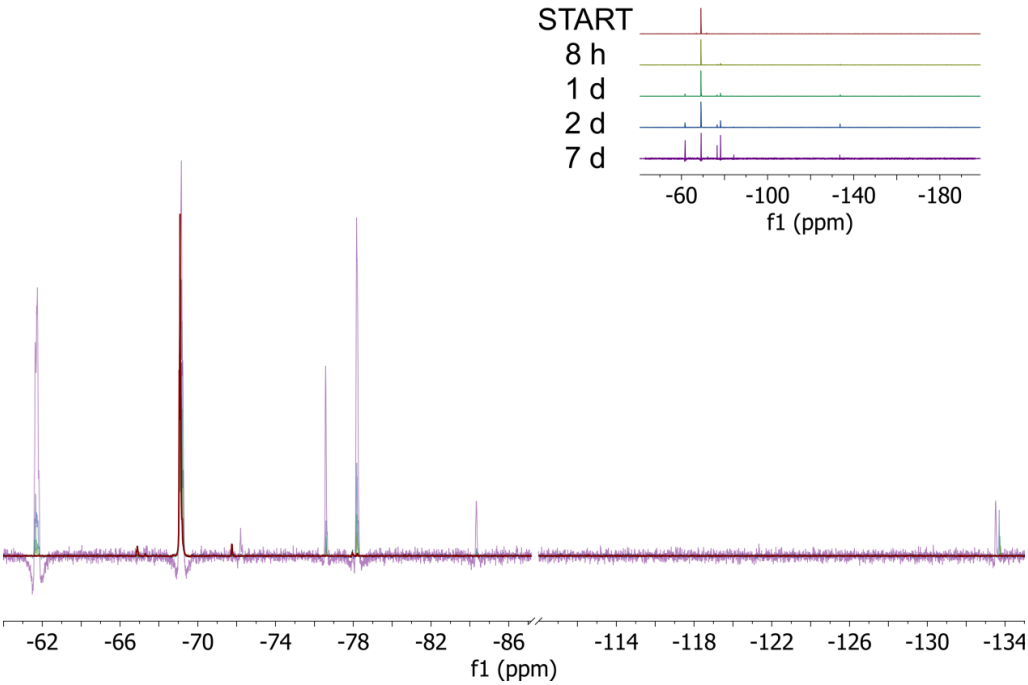

Figure S28. ^{19}F NMR spectra showing hydrolytic stability of **14** in a strongly alkaline solution (pH 11). 282 MHz, 25 °C. No C–F cleavage was observed, but a different decomposition route was observed.

Trial to hydrolyse 15

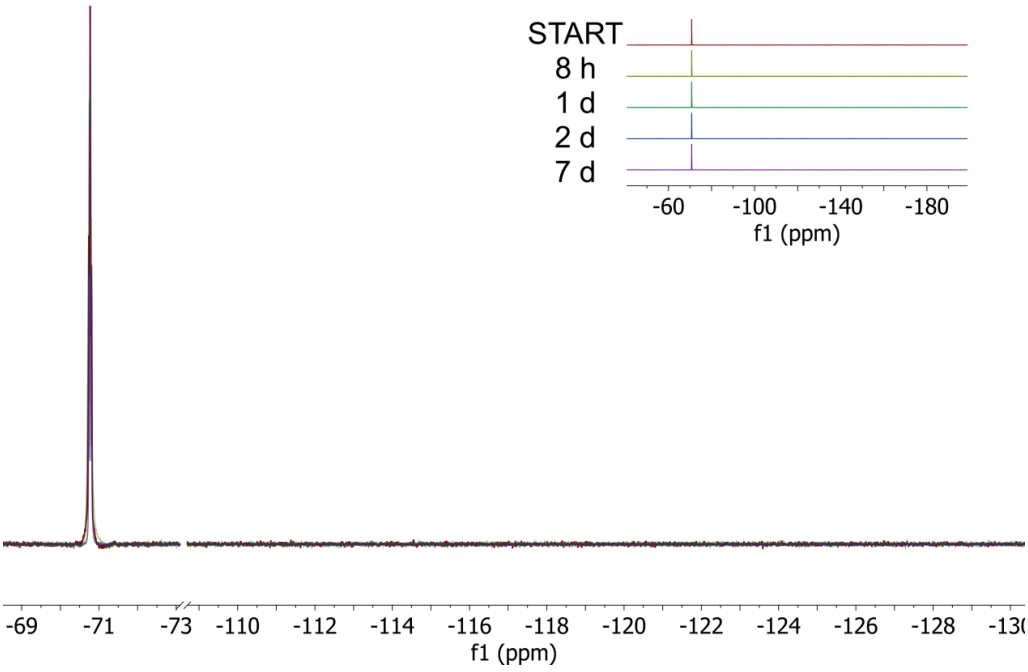

Figure S29. ^{19}F NMR spectra showing hydrolytic stability of **15** in a strongly alkaline solution (pH 11). 282 MHz, 25 °C.

Trial to hydrolyse 16

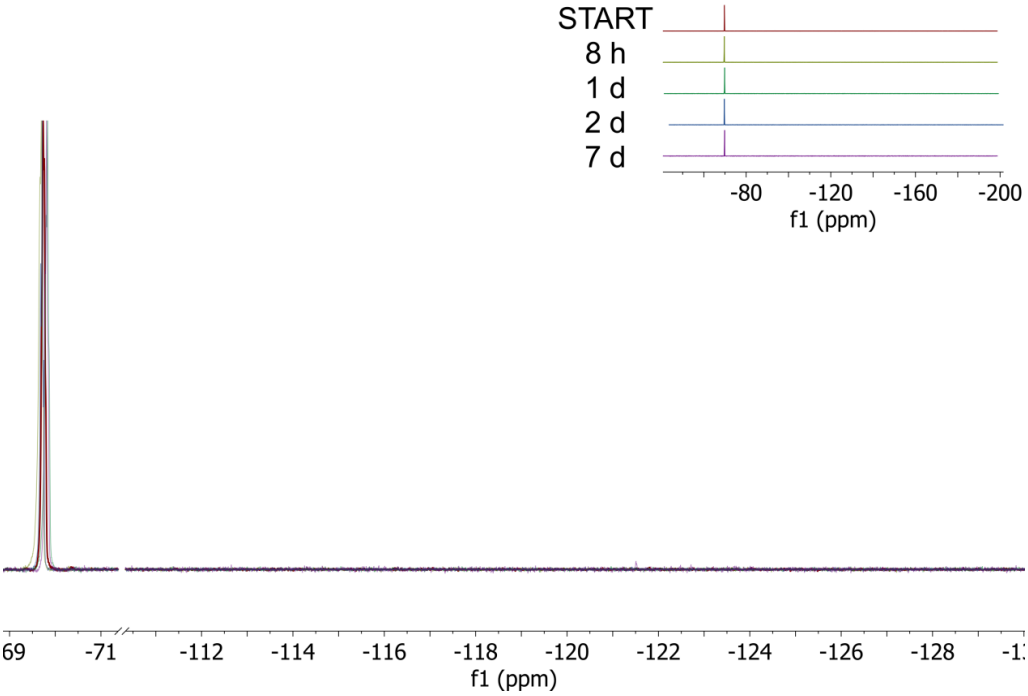

Figure S30. ^{19}F NMR spectra showing hydrolytic stability of **16** in a strongly alkaline solution (pH 11). 282 MHz, 25 °C.

Characterisation of the product of the hydrolysis of 1: carboxymethylphosphinic acid 18

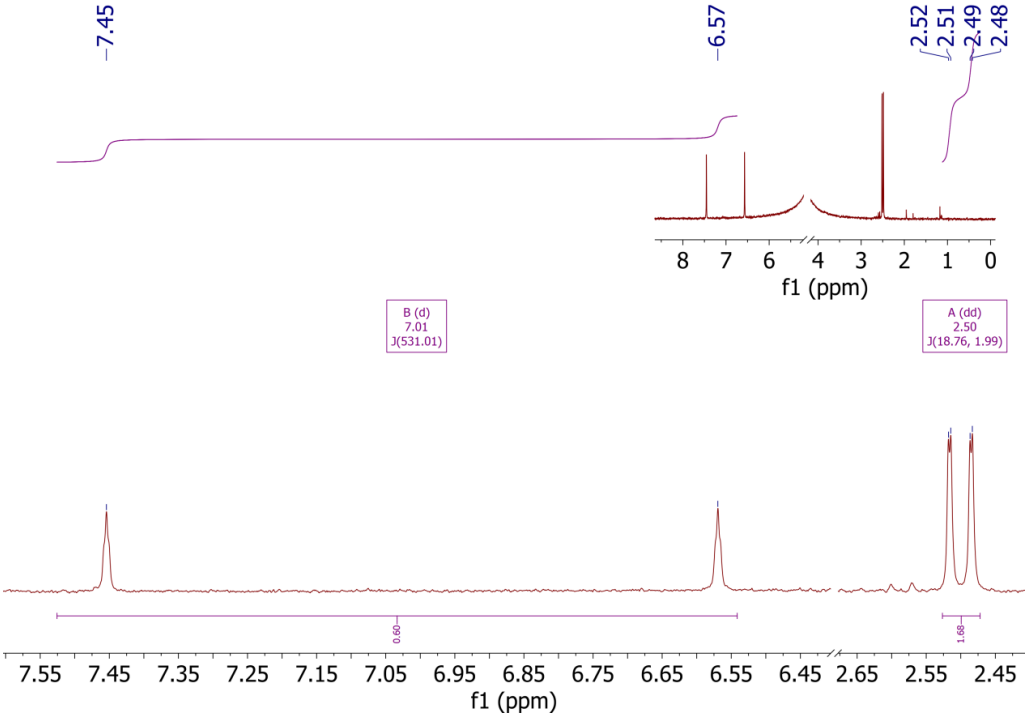

Figure S31. ^{1}H NMR spectrum of **18**. 600 MHz, 25 °C, H_2O, pH > 11.

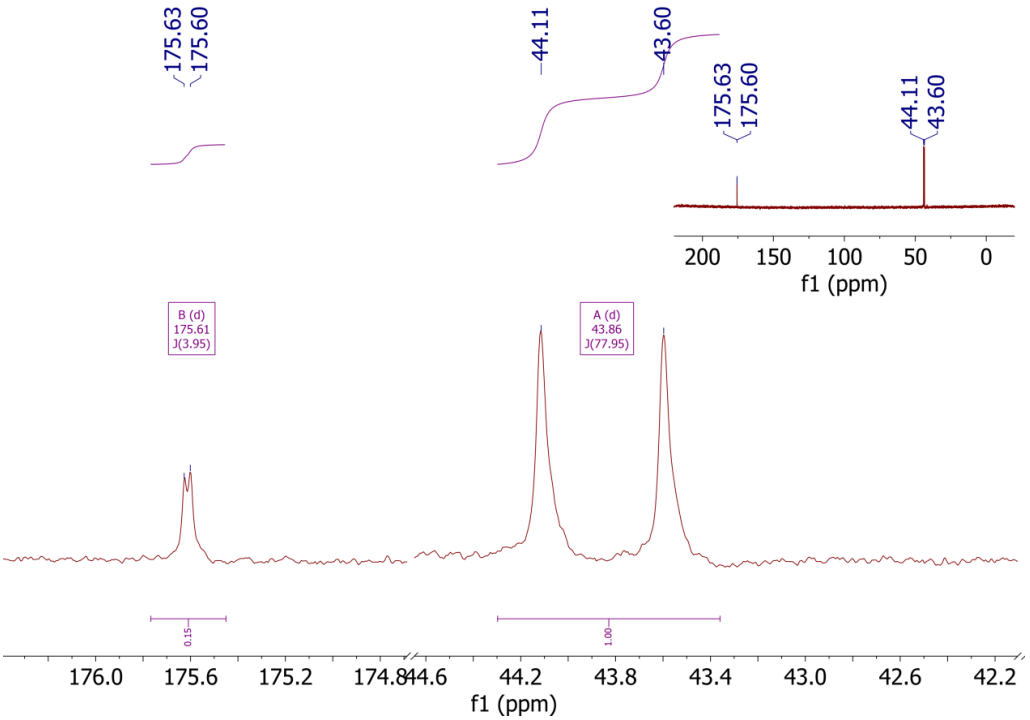

Figure S32. ^{13}C{^{1}H} spectrum of **18**. 151 MHz, 25 °C, H_2O, pH > 11.

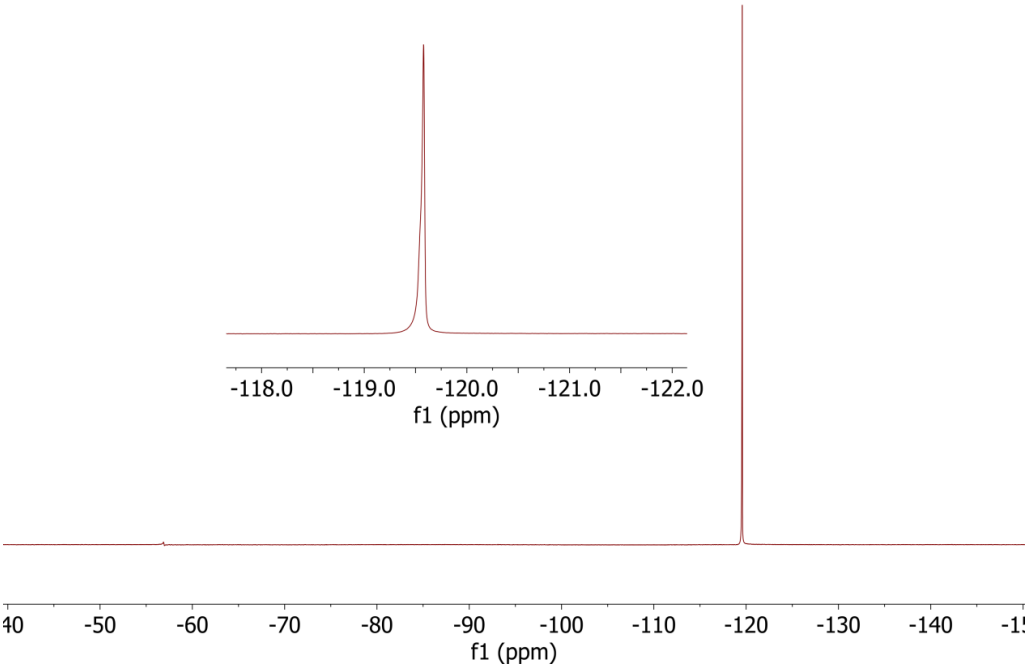

Figure S33. ^{19}F NMR spectrum of hydrolysed **1**. 282 MHz, 25 °C, H_2O, pH > 11. No remaining **1** was observed, the signal at ca −120 ppm corresponds to F^-.

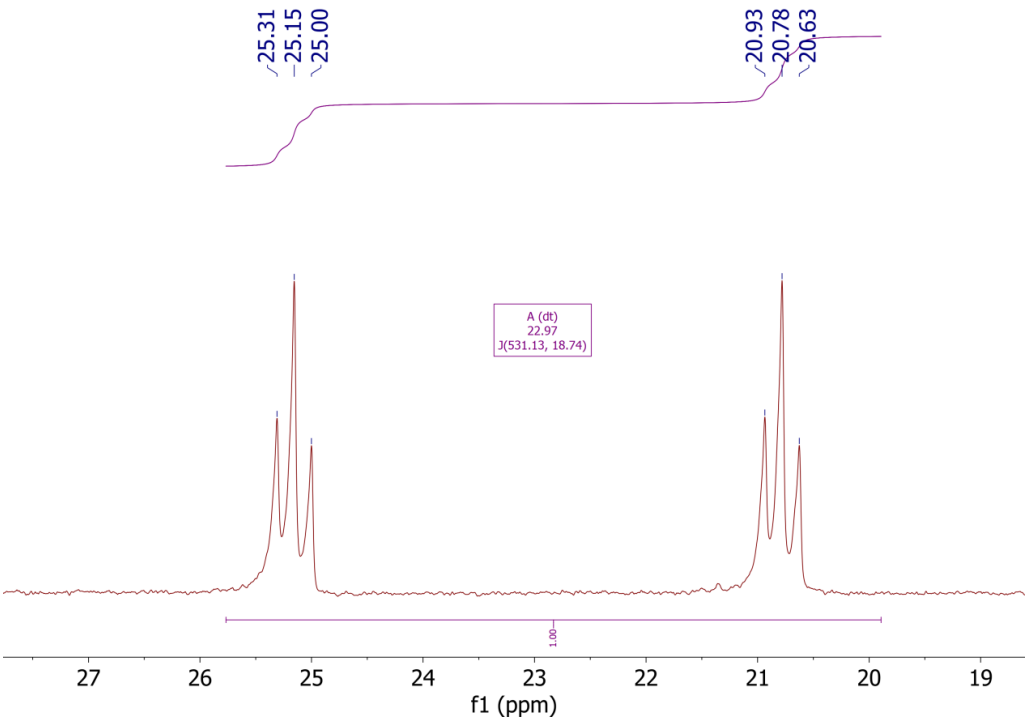

Figure S34. ^{31}P NMR spectrum of **18**. 121 MHz, 25 °C, H_2O, pH > 11.

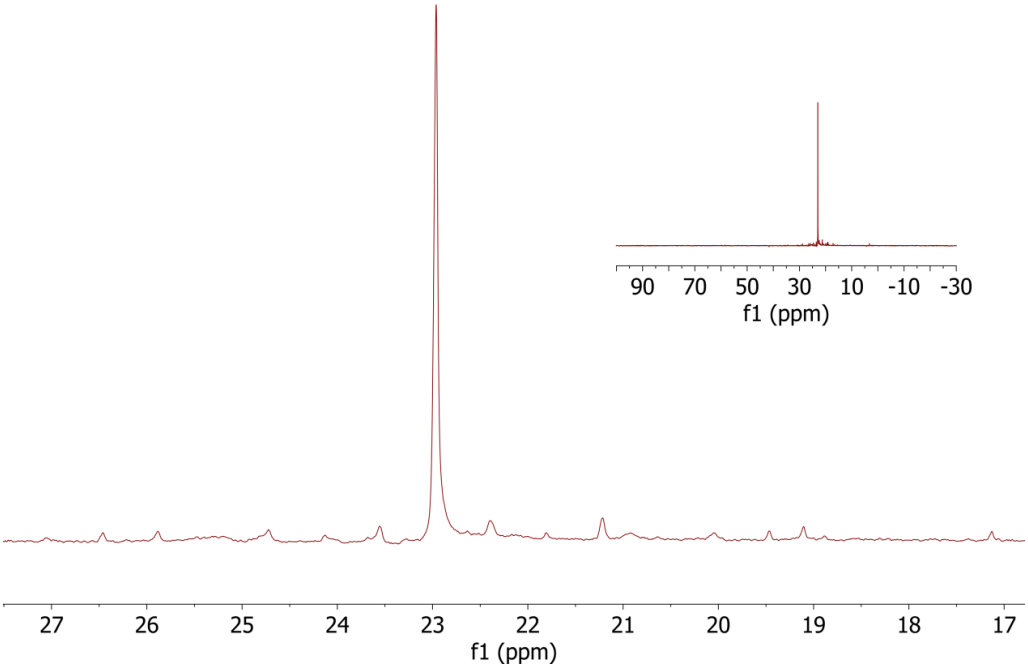

Figure S35. $^{31}P\{^{1}H\}$ NMR spectrum of **18**. 121 MHz, 25 °C, H_2O, pH > 11.

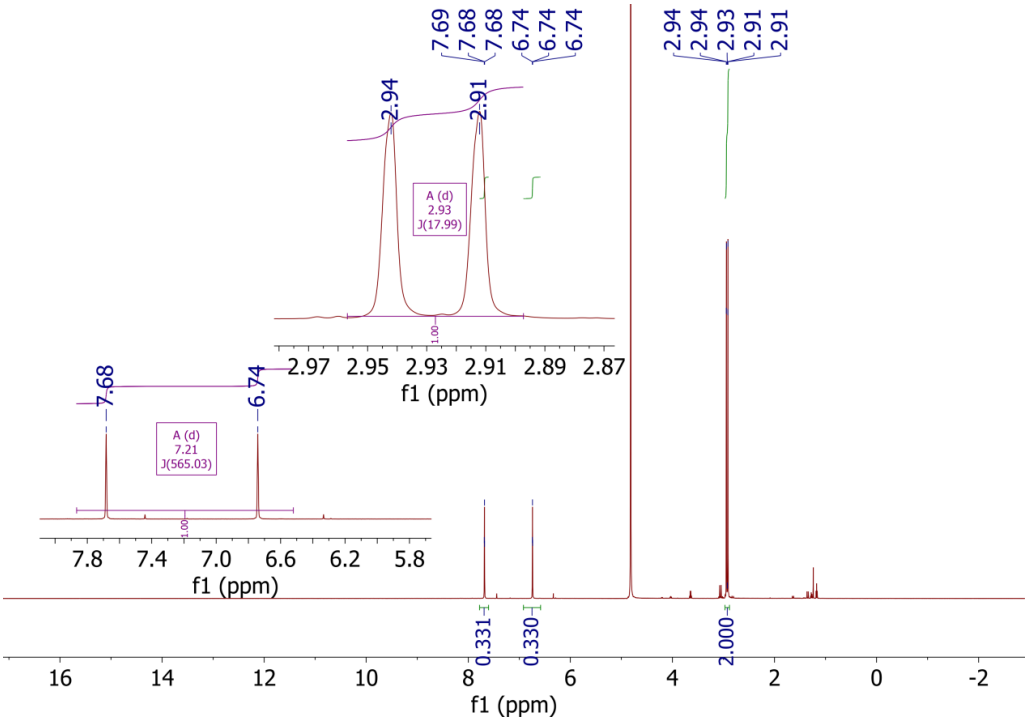

Figure S36. ^{1}H NMR spectrum of **18**. 600 MHz, 25 °C, D_2O, pH 0.9.

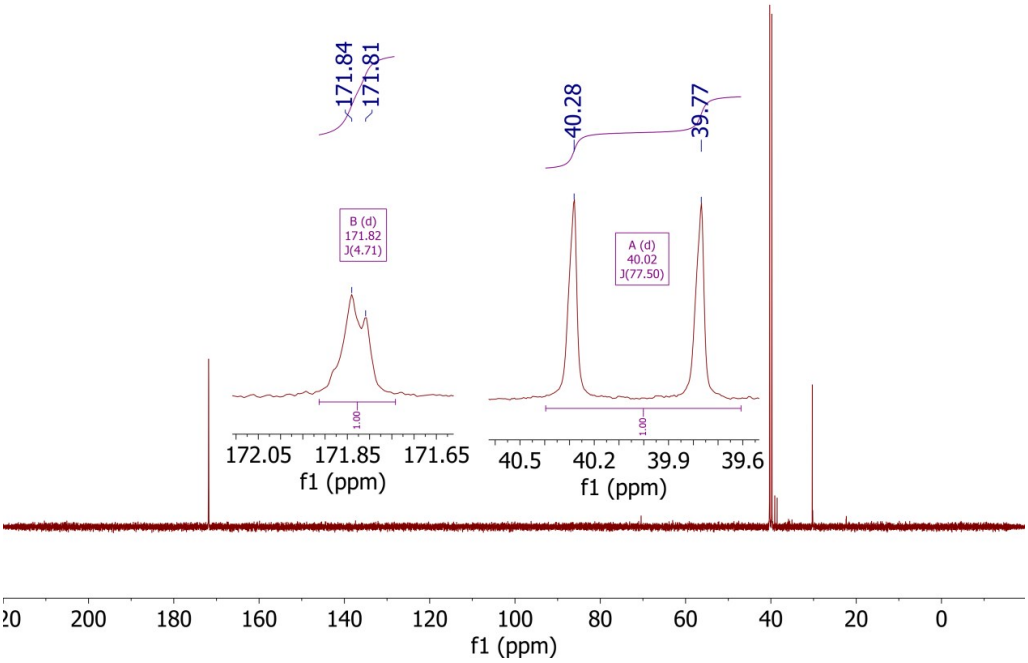

Figure S37. $^{13}C\{^{1}H\}$ NMR spectrum of **18**. 151 MHz, 25 °C, D_2O, pH 0.9.

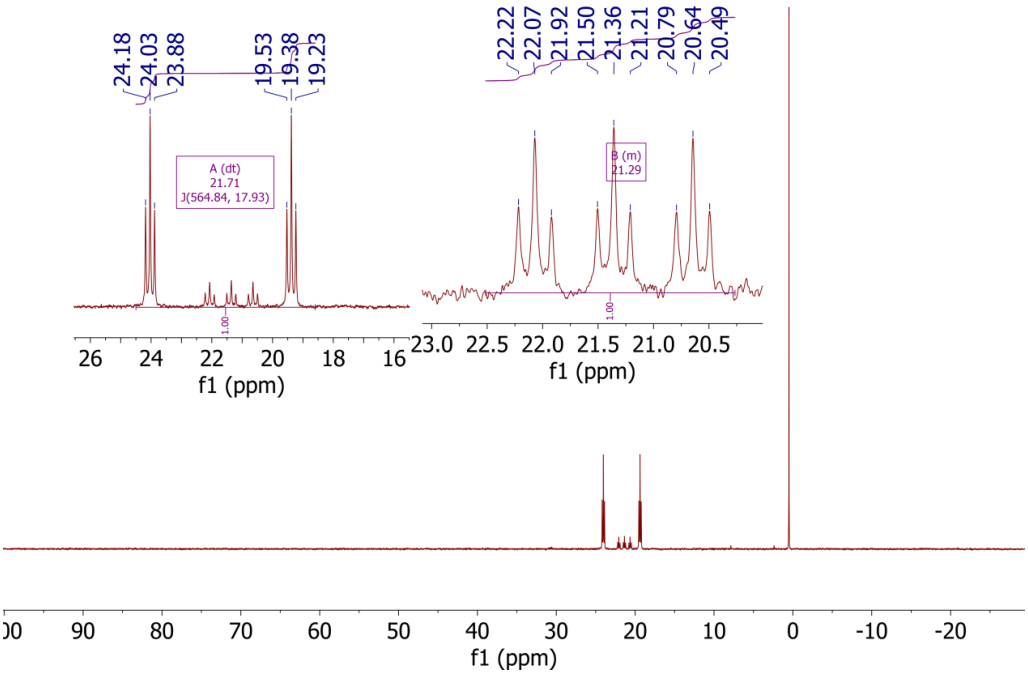

Figure S38. ^{31}P NMR spectrum of **18**. 121 MHz, 25 °C, D_2O, pH 0.9.

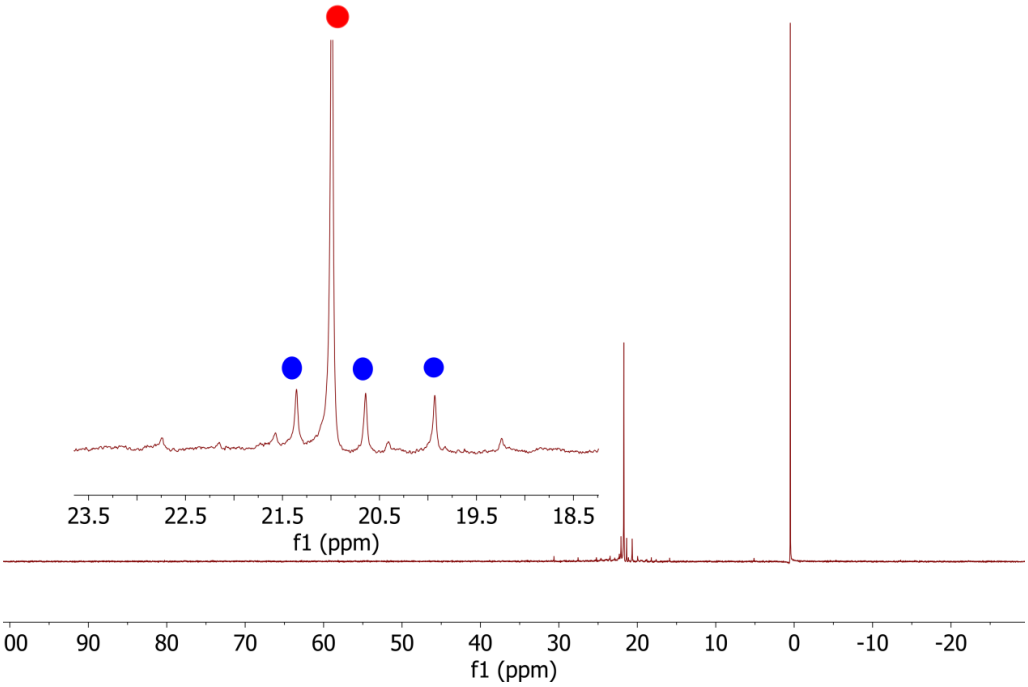

Figure S39. $^{31}P\{^{1}H\}$ NMR spectrum of **18**. 121 MHz, 25 °C, D_2O, pH 0.9. Red-labelled signal corresponds to species with the P–H bond, blue–labelled signals correspond to species with P–D bond.

Experimental crystallographic details

Diffraction data were collected using a Bruker APEX-II CCD diffractometer (compound **17**) at 150 K using Mo-Kα (λ = 0.71073 Å) radiation or on a Bruker D8 VENTURE Kappa Duo PHOTON100 diffractometer at 120 K (**16**·HCl, **19**·2H_2O) using Mo-Kα radiation or 100 K (NH_3·**6**) using Cu-Kα (λ = 1.54178 Å) radiation. Data were analysed using the SAINT (Bruker AXS Inc.) software package and subsequently corrected for absorption effects using the numerical method (SADABS).[6] The structures were solved using direct methods (SHELXT2018)[7] and refined with full-matrix least-squares techniques (SHELXL2017).[8]

All non-hydrogen atoms were refined anisotropically. All hydrogen atoms were found in the difference density map. However, the hydrogen atoms bound to the carbon atoms were fixed in theoretical positions using U_{eq}(H) = 1.2 U_{eq}(C) to keep the number of refined parameters low, and the hydrogen atoms bound to the oxygen or nitrogen atoms were usually fixed in the original position of electron maxima as their full refinement led to unrealistic bond lengths due to hydrogen bonds.

In the crystal structure of NH_3·**6**, two formula units form the structurally independent unit. In the crystal structure of **16**·HCl, one molecule forms the structurally independent unit, and the nitrogen-bound hydrogen atom was fully refined. The trifluoromethyl group was refined disordered in two positions with relative occupancies of 59:41%. In the crystal structure of **17**, one molecule forms the

structurally independent unit. One of the trifluoroethyl groups was refined disordered in two positions with relative occupancies of 83:17%. In the crystal structure of **19**·2H_2O, the molecule of **19** is centrosymmetric, and the independent part is thus formed by one half of the formula unit. The nitrogen-bound hydrogen atom was fully refined. An overview of the experimental data is compiled in Table S1.

Table S1. Experimental data of reported crystal structures.

	NH_3·**6**	**16**·HCl	**17**	**19**·2H_2O
Empirical formula	$C_2H_7F_3NO_3P$	$C_6H_{11}ClF_3NO$	$C_9H_{15}F_9NO_6P_3$	$C_{16}H_{36}CuN_4O_{10}P_2$
Formula weight	181.06	205.61	497.13	569.97
Crystal system	monoclinic	triclinic	triclinic	triclinic
Space group	*Cc*	*P*–1	*P*–1	*P*–1
a, Å	10.8639(11)	6.9673(7)	8.9880(2)	8.1026(7)
b, Å	23.001(2)	8.4006(8)	9.1058(2)	8.8622(7)
c, Å	7.7886(14)	8.7777(9)	13.0820(3)	9.2776(8)
α, °	90	61.809(3)	77.811(1)	71.336(3)
β, °	133.943(2)	83.564(3)	74.437(1)	65.675(3)
γ, °	90	84.306(3)	61.391(1)	79.661(3)
Volume, Å3	1401.3(3)	449.33(8)	497.13	574.25(9)
Z	8	2	2	1
Reflections collected	2251	2604	4095	2627
Independent reflections	2230	2557	3542	2417
R(I>2σ(I))	0.0548	0.0216	0.0374	0.0485
R'(all data)	0.0555	0.0219	0.0440	0.0526
wR(I>2σ(I))	0.1463	0.0601	0.0975	0.1350
wR'(all data)	0.1483	0.0613	0.1024	0.1418
CCDC number	2489254	2489252	2489253	2489251

References

[1] K. G. Andrews, R. Faizova and R. M. Denton, A practical and catalyst-free trifluoroethylation reaction of amines using trifluoroacetic acid, *Nature Commun.*, 2017, **8**, 15913. DOI: 10.1038/ncomms15913.

[2] M. Epifanov, P. J. Foth, F. Gu, C. Barrillon, S. S. Kanani, C. S. Higman, J. E. Hein and G. M. Sammis, One-pot 1,1-dihydrofluoroalkylation of amines using sulfuryl fluoride, *J. Am. Chem. Soc.*, 2018, **140**, 16464–16468. DOI: 10.1021/jacs.8b11309.

[3] E. Abedelnour, S. Ognier, O. Venier, L. Schio, M. Tatouliana and J. Cossy, Synthesis of trifluoromethyl *N*,*N*-aminals from nitrogen containing heterocycles by using a plasma flow microreactor, *Chem. Commun.*, 2023, **59**, 4213–4216. DOI: 10.1039/d3cc00942d.

[4] J. Blahut, P. Hermann, A. Gálisová, V. Herynek, I. Císařová, Z. Tošner and J. Kotek, Nickel(II) complexes of *N*-CH_2CF_3 cyclam derivatives as contrast agents for ^{19}F magnetic resonance imaging, *Dalton Trans.*, 2016, **45**, 474–478. DOI: 10.1039/C5DT04138D.

[5] Z. Kotková, F. Koucký, J. Kotek, I. Císařová, D. Parker and P. Hermann, Copper(II) complexes of cyclams with *N*-(2,2,2-trifluoroethyl)-aminoalkyl pendant arms as potential probes for ^{19}F magnetic resonance imaging, *Dalton Trans.*, 2023, **52**, 1861–1875. DOI: 10.1039/D2DT03360G.

[6] L. Krause, R. Herbst-Irmer, G. M. Sheldrick and D. Stalke, Comparison of silver and molybdenum microfocus X-ray sources for single-crystal structure determination, *J. Appl. Cryst.*, 2015, **48**, 3–10. DOI: 10.1107/S1600576714022985.

[7] G. M. Sheldrick, SHELXT2018/2. Program for Crystal Structure Solution from Diffraction Data, University of Göttingen, Göttingen, 2018.

[8] G. M. Sheldrick, SHELXL-2017/1. Program for Crystal Structure Refinement from Diffraction Data, University of Göttingen, Göttingen, 2017.